

Multi-channel transmitters for free-space optical communication systems

Aleksandra Paśnikowska^{1*}, Stanisław Stopiński^{1,2,3}, Krzysztof Anders^{1,2,3},
Mariusz Rojewski¹, Łukasz Kustos¹ and Ryszard Piramidowicz^{1,2,3}

¹ *Warsaw University of Technology, Institute of Microelectronics and Optoelectronics,
ul. Koszykowa 75, 00-662 Warsaw, Poland*

² *VIGO Photonics S.A., Poznańska 129/133, 05-850 Ożarów Mazowiecki, Poland*

³ *LightHouse sp. z o.o., Stefczyka 34, 20-151 Lublin, Poland*

Received January 01, 2026; accepted March 30, 2026; published March 31, 2026

Abstract—This study presents a Free Space Optical Communication system using InP-based integrated transceivers, demonstrating multichannel transmission capabilities. The system utilizes photonic integrated circuits (PICs) to achieve compact, energy-efficient transceivers suitable for scalable optical communication applications. Successful multi-channel data transmission at rates of up to 10 Gb/s was achieved in both indoor (2 m) and outdoor (up to 10 m) environments. The design incorporates distributed Bragg reflector (DBR) lasers, electro-absorption modulators, and arrayed waveguide grating (AWG) multiplexers. The system showcases high-quality transmission with low bit-error rates ($BER \leq 10^{-11}$) and minimal power penalties.

Free Space Optical Communication (FSOC) is a cutting-edge wireless communication technology that enables the transmission of data through free space, such as air or vacuum. Unlike traditional fiber-optic systems, FSOC requires no physical cables, thus enabling faster deployment, greater flexibility, and scalable connectivity across a wide range of applications.

FSOC offers several advantages over other communication technologies. It operates on unlicensed frequency bands, avoiding spectrum congestion, and provides high data rates, while remaining free from electromagnetic interference. Additionally, FSOC systems are energy-efficient, providing low latency and enhanced security due to their low beam divergence, which makes eavesdropping highly challenging. These features make FSOC an ideal solution for applications that require high bandwidth, low power consumption, and secure data transmission.

FSOC technology is widely used across multiple domains, offering a cost-effective alternative to deploying optical fiber for last-mile connectivity in urban areas and enabling seamless integration with existing optical backbones. It is also used to establish or extend Local and Metropolitan Area Networks (LANs/MANs), particularly when rapid deployment is required. FSOC plays a critical

role in satellite-based uplinks and downlinks in remote regions, as demonstrated by systems such as SpaceX Starlink, which supports ground-to-satellite, satellite-to-satellite, and air-to-ground communication [1].

FSOC's ability to be rapidly deployed and to operate independently of existing infrastructure makes it invaluable during emergencies or other temporary events. This was clearly demonstrated after the attack on the World Trade Center, when FSOC links helped alleviate communication bottlenecks [2]. Its high bandwidth, rapid deployment, and strong security make it also suitable for military applications, including terrestrial operations, air-to-ground links, and unmanned aerial vehicle steering (UAV). Furthermore, FSOC is well-suited for deep-space communication [3] and can be effectively applied in data centers, enabling high-capacity, low-latency, and interference-free optical links between buildings or racks, offering a flexible alternative or complement to fiber-optic connections [4].

Recent advancements in FSOC technology have substantially expanded achievable performance, as evidenced by demonstrations of 20 Gb/s transmission over 1 km at 1550 nm [4] or 100 Gb/s over short distances in the L-band [5]. In parallel, the development of systems operating in the Mid-Wave Infrared (MWIR) and Long-Wave Infrared (LWIR) spectral regions offers enhanced robustness against atmospheric effects, enabling more stable operation under challenging outdoor conditions [6]. Consequently, FSOC is increasingly recognized as a versatile, high-performance candidate for next-generation communication networks.

This work investigates the applicability of Photonic Integrated Circuits (PICs) to FSOC systems. PICs enable the development of free-space multichannel transceivers, offering advantages in terms of footprint, reliability, energy efficiency, and cost [7-10].

* E-mail: aleksandra.pasnikowska@pw.edu.pl



The free-space optical communication link was implemented using an integrated multi-channel transmitter (Tx) and an integrated receiver (Rx). Both devices were realized using generic InP-based photonic integration technology in a fabless model. The transmitter circuit and mask layout are shown in Fig. 1. Four-section CW DBR lasers serve as the light sources. Each laser comprises tunable Bragg gratings as rear and front mirrors, a semiconductor optical amplifier (SOA), and a phase-control section for fine-tuning the wavelength. Digital signal modulation is provided by electro-absorption modulators (EAMs). A cyclic arrayed waveguide grating (AWG) is used to multiplex all channels. The chip outputs are connected to spot-size converters that provide a low-loss interface (ca. 2.0 dB) with a standard single-mode fiber. The integrated receiver comprises a PIN photodiode. The fabricated chips measure $4 \times 6 \text{ mm}^2$. Further details on the fabrication technology and the design of both the transmitter and receiver are provided in [8].

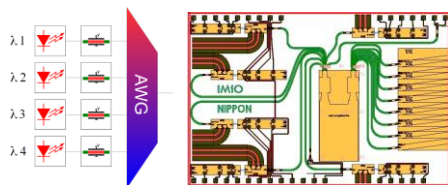


Fig. 1. a) Circuit scheme, b) mask layout of the integrated multi-channel transmitter.

Tx and Rx chips were assembled using either a chip-on-board submount or a gold-box packaging scheme (Fig. 2a), each providing a convenient electrical and optical interface as well as temperature control.

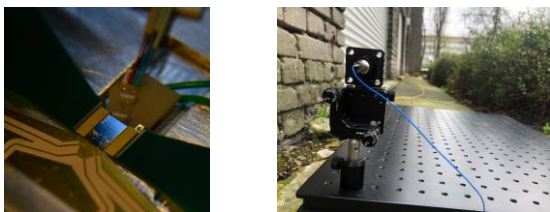


Fig. 2. Photograph of a) the integrated transmitter, b) the outdoor FSOC link setup.

The measured wavelengths of the four channels are 1577.0 nm (CH1), 1577.7 nm (CH2), 1578.5 nm (CH3), and 1579.4 nm (CH4). The channel spacing ($0.8 \pm 0.1 \text{ nm}$) aligns well with the AWG multiplexer design value ($\Delta\lambda = 0.8 \text{ nm}$). The laser threshold current is approximately 20 mA, and the maximum output power reaches $250 \mu\text{W}$. Additionally, the measured extinction ratio of the electro-absorption modulators is 25 dB at a driving voltage of 4.0 V.

Digital transmission tests were conducted both indoors under laboratory conditions and outdoors at a maximum distance of 10 m. The measurement setup used in the experiments is shown in Fig. 3.

The DBR lasers of the integrated multichannel transmitter were driven by standard laser diode drivers operating at currents ranging from 130 mA to 160 mA. The electro-absorption modulators were driven using an electrical pattern generator (pseudo-random bit sequence, PRBS, bit rate between 2.5 Gb/s and 10 Gb/s, word length $2^{31}-1$). The RF signal was amplified and connected through a bias-tee (BT) to the EAM, together with a DC bias supplied by a precise source-measure unit (SMU). The photonic chip was thermally stabilized at 20°C .

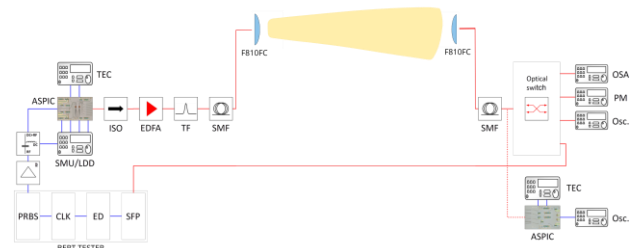


Fig. 3. Scheme of the measurement setups.

The optical output of the transmitter was routed through an isolator (ISO), an L-band erbium-doped fiber amplifier (EDFA), and a tunable filter (TF) to a fiber collimator (Thorlabs F810FC) mounted on a three-axis positioner. The signal was collected on the other side of the free-space link by another F810FC collimator. The signal was then launched directly to the integrated receiver (ASPIC) or, through an optical switch, to an optical spectrum analyzer (OSA), an optical power meter (PM), a digital sampling oscilloscope (Osc.), or an SFP transceiver module. The latter served as the optoelectronic interface for the mainframe of the BER tester.

First, the transmission parameters over a short distance ($d = 2 \text{ m}$) were evaluated under laboratory conditions. In Fig. 4, the eye diagrams recorded with the sampling oscilloscope are presented. In this case, the ASPIC was used as the receiver. The bit rates of the modulation signal were 2.5 Gb/s, 5.0 Gb/s, and 10 Gb/s, respectively. The measured time traces confirm the good quality of the transmission – the eyes are open, and the dynamic extinction ratio is between 4 and 6 dB.

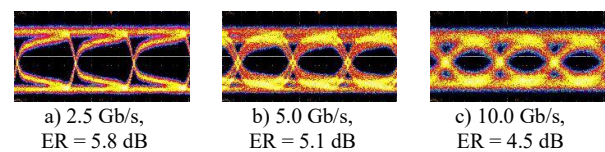


Fig. 4. Recorded eye diagrams for a free-space link over a distance of 2 m (indoor, laboratory conditions) at modulation speeds 2.5-10 Gb/s.

Secondly, direct bit-error rate (BER) measurements were performed using the SFP+ module installed in the BER testing system. In Fig. 5, the determined BER values as a function of the received optical power are presented. The incident power was controlled by an optical attenuator integrated into the optical switch. The reference values (back-to-back, BTB) were obtained when the transmitter and receiver were connected directly via optical fibers, i.e., without free-space propagation.

The best measured BER values for each modulation speed reached 10^{-11} . The measurement was repeated under different transmission channel conditions, i.e., with a single channel or two channels enabled simultaneously. No significant influence of the second channel on transmission quality was observed – the power penalty at $\text{BER} = 10^{-11}$ was merely 1.0 dB, and only in the case of two adjacent channels (CH3+CH4).

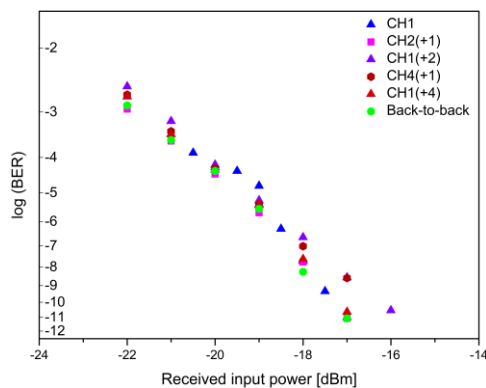


Fig. 5. BER characteristics as a function of optical power for single and multichannel transmission over 2 m under laboratory conditions.

Similar tests were conducted outdoors under clear weather conditions (temperature of 16°C , no rain, no fog, in the afternoon) (Fig. 3b). In Fig. 6, a recorded eye diagram for the 10 Gb/s signal over a 10 m distance is presented. The eye is open, and the dynamic ER is as good as 4.3 dB.

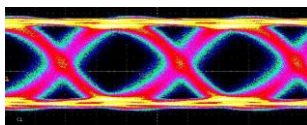


Fig. 6. Recorded eye diagram for a 10 Gb/s free-space link over a distance of 10 m in outdoor conditions.

Outdoor BER measurements were also performed. The BER characteristics are shown in Fig. 7. The signal was generated by the ASPIC transmitter and received by an SFP+ module. Modulation speeds of 5 Gb/s, 10 Gb/s, and 15 Gb/s were tested. Although the highest bit rate requires significantly more power (a power penalty of 16 dB at 10 Gb/s), BER values as low as 10^{-11} were recorded.

We demonstrated the transmission capabilities of an ASPIC-based FSOC system employing integrated multichannel transceivers. The system supports data rates

ranging from 2.5 to 15 Gb/s over short- to medium-range distances of 2–10 m under both indoor and outdoor conditions. Experimental results confirm that photonic integrated circuits can be effectively applied to FSOC systems. The demonstrated free-space link exhibits stable operation, characterized by open eye diagrams and BER values as low as 10^{-11} . These results highlight the potential of integrated photonic solutions to advance FSOC technology for urban, military, and satellite communication applications.

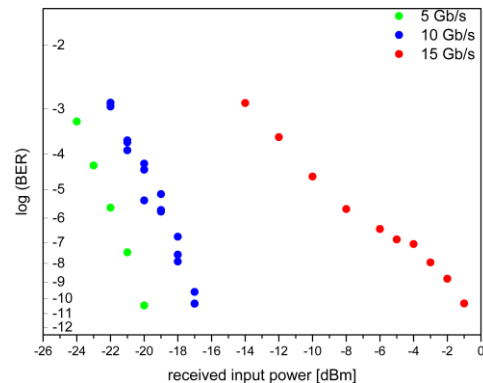


Fig. 7. BER characteristics as a function of optical power for outdoor transmission over 10 m at data rates from 5 to 15 Gb/s.

This research was funded by (POB Photonics) of Warsaw University of Technology within the Excellence Initiative: Research University (IDUB) program – project “Photonic integrated circuits for applications in free-space optical communication systems”(504/04496/1035/45.010109) and under FENG – 1.1, project “Integrated Photonics Systems for Free-Space Optical Communication (FSOC)” FENG.01.01-IP.01-A0MR/24.

References

- [1] H. Kaushal and G. Kaddoum, *IEEE Commun. Surv. Tutor.* **19**(1), 57 (2017), doi: 10.1109/COMST.2016.2603518.
- [2] *Free-space optics restores communications after Sept. 11*, Lightwave Online, accessed: Dec. 23, 2025. [Online]. Available: <https://www.lightwaveonline.com/optical-tech/article/16648109/free-space-optics-restores-communications-after-sept-11>
- [3] H. Hemmati, A. Biswas, I.B. Djordjevic, *Proc. IEEE* **99**(11), 2020 (2011), doi: 10.1109/JPROC.2011.2160609.
- [4] *Free-Space Terabit Optical Interconnects*, accessed: Dec. 31, 2025. [Online]. Available: <https://ieeexplore-ieee-org-1zrbhrpc60005.eczyt.bg.pw.edu.pl/document/9640495>
- [5] H. Zhao *et al.*, *IEEE J. Sel. Top. Quantum Electron.* **24**(6), 1 (2018), doi: 10.1109/JSTQE.2018.2866677.
- [6] G. Terrasanta, M.W. Ziarko, N. Bergamasco, M. Poot, J. Poliak, *Int. J. Satell. Commun. Netw.* **43**(3), 210 (2025), doi: 10.1002/sat.1552.
- [7] L.A. Coldren *et al.*, *J. Light. Technol.* **29**(4), 554 (2011), doi: 10.1109/JLT.2010.2100807.
- [8] A. Pańnikowska, S. Stopiński, A. Kaźmierczak, R. Piramidowicz, *J. Light. Technol.* **42**(7), 2371 (2024), doi: 10.1109/JLT.2023.3339594.